An International Journal of Computational Thermal Sciences, vol. 1, pp. xx–xx, 2009

A MULTISCALE FULL-SPECTRUM k-DISTRIBUTION METHOD FOR RADIATIVE TRANSFER IN NONHOMOGENEOUS GAS–SOOT MIXTURES WITH WALL EMISSION

Gopalendu Pal and Michael F. Modest

Department of Mechanical and Nuclear Engineering, The Pennsylvania State University, University Park, PA, USA

The multiscale full-spectrum k-distribution (MSFSK) method has become a promising method for radiative heat transfer in inhomogeneous media. The scope of the MSFSK method has been limited to radiation calculations involving inhomogeneous gas mixtures only. The objective of this paper is to develop a MSFSK model that is accurate for inhomogeneous mixtures of both gases and nongray particles, such as soot. Soot is added as one more scale in addition to the gas scales. The overlap parameters between scales are calculated by mixing molecular gases with soot particles at the narrowband level. This MSFSK method is also capable of black/gray wall emission. Because wall emission is continuous over the spectrum, similar to radiation from soot, wall emission is treated within the soot scale. Sample calculations are performed for a one-dimensional medium with step changes in species concentration and temperature and also for a two-dimensional axisymmetric medium involving combustion of methane. The MSFSK method is observed to accurately predict heat transfer from inhomogeneous gas–soot mixture with/without wall emission yielding close to line-by-line accuracy with several orders of magnitude less computational cost.

INTRODUCTION

Radiative transfer calculations in participating media by the line-by-line (LBL) approach is the most accurate yet extremely time-consuming and requires large computer resources. For accurate and computationally efficient solutions of radiative transfer equation (RTE), several models have been proposed applying the concept of reordering the absorption coefficient to the entire spectrum, and these include the spectral-line-based weighted-sum-of-gray-gases (SLW) model (Denison and Webb, 1993, 1995), the absorption distribution function (ADF) method (Rivière et al., 1996; Pierrot et al., 1999), and full-spectrum k-distribution (FSK) method (Modest and Zhang, 2002). Whereas SLW and ADF methods are approximate schemes, in which the absorption coefficient is reduced to a few discrete values, the FSK method is an exact method for a correlated absorption coefficient using a continuous k-distribution over the entire spectrum. Although the FSK scheme is an exact method for radiative calculations in homogeneous

Correspondence concerning this article should be addressed to Michael F. Modest, Department of Mechanical and Nuclear Engineering, The Pennsylvania State University, University Park, PA, USA; e-mail:mfmodest@psu.edu.

ISSN 1940-2503/09/35.00

media, its application in strongly inhomogeneous emitting-absorbing media challenges its accuracy. One additional shortcoming of the FSK method is that it is impossible to assemble k-distributions for a gas mixed with nongray absorbing particles (such as soot) from gas-only full-spectrum k-distributions.

Several advancements to the k-distribution method have been proposed to address the shortcomings of the basic FSK scheme. The advanced k-distribution methods with their advantages and shortcomings are summarized in Table 1. Two different approaches, namely, the fictitious gas (FG) (Pierrot et al., 1999) or multiscale (Zhang and Modest, 2002) approach and the multi-group (MG) approach (Zhang and Modest, 2003a,b) were proposed to alleviate inaccuracies due to inhomogeneities in gas mixtures. In the fictitious gas approach, the individual spectral lines comprising the absorption coefficient are placed into separate scales based on their temperature dependence. In the multigroup approach, spectral positions (i.e., wavenumbers) are placed into several groups according to their dependence on temperature and partial pressure. The multigroup FSK (MGFSK) method has been shown to achieve great accuracy for a single gas species with inhomogeneity in temperature (Zhang and Modest, 2002, 2003a,b), whereas the multiscale FSK (MSFSK) method can efficiently treat mixtures of absorbing gases with severe species inhomogeneity (Wang and Modest, 2005). Combining the advantages of both the methods, a hybrid multiscale multigroup FSK (MSMGFSK) method has been developed that can handle radiation from a gas mixture with both temperature and concentration inhomogeneity (Pal and Modest, 2007; Pal et al., 2007). For radiation calculations in a multiphase mixture, nongray soot particles were mixed with the molecular gases within the framework of the narrowband-based single-scale FSK method by Modest and Riazzi (2004). But challenges still remain for radiative calculations in an inhomogeneous gas mixture containing nongray soot.

Soot radiation constitutes an important part of radiation calculations in luminous flames. Because of the difficulties in soot modeling, soot radiation in combustion flames has been treated commonly using the optically thin approximation with the assumption of gray soot (Wang et al., 2005). Previously, nongray soot has been investigated by Solovjov and Webb (2001) using the SLW method and by Wang et al., who employed the single-scale FSK method (Wang et al., 2005). Solovjov and Webb treated nongray soot as an additional nongray gas species and the multi-component gas mixture with soot was treated as a single gas within the SLW method. To include nongray soot in the single-scale FSK method (Wang et al., 2005), the local mixture k-g-distributions, consisting of contributions from gas-phase species and soot particles, can be constructed in two ways: *(i)* by summing the gas-phase and soot absorption coefficients in an LBL manner from spectroscopic databases and *(ii)* by mixing precalculated single-gas k-distributions (SGKs) according to the local gas mixture composition. The contribution from soot particles is then incorporated into the local gas mixture k-g-distributions. Although the first method is computationally intensive, the second method can produce local k-g-

Table 1. Advanced k-distribution methods

Method	Advantages	Shortcomings
Single-scale FSK (8–10 RTEs) (Modest and Zhang, 2002)	Most CPU efficient; Accurate for moderately inhomogeneous media	Inaccurate for strongly inhomogeneous media; problems with mixing of species
Narrowband based single-scale FSK (8–10 RTEs) (Modest and Riazzi, 2004)	Most CPU efficient; mixing of multiphase species; accurate for moderately homogeneous media	Inaccurate for strongly inhomogeneous media
Multiscale FSK/ fictitious gas $N\times$(8–10) RTEs (Pierrot et al., 1999; Zhang and Modest, 2002)	Accurate for mixing and species (gas only) inhomogeneity	Inaccurate for strong temperature inhomogeneity and multiphase mixing
Multigroup FSK $M\times$(8–10) RTEs (Zhang and Modest, 2003a,b)	Accurate for temperature inhomogeneity in a single gas	No mixing of species; inaccurate for species inhomogeneity
Narrowband-based multiscale FSK $N\times$(8–10) RTEs (Wang and Modest, 2005a)	Better accuracy for mixing of gases than MSFSK; potential for multiphase mixing	Inaccurate for strong temperature inhomogeneity
Multiscale multigroup FSK $N \times M\times$(8–10) RTEs (Pal and Modest, 2007; Pal et al. 2007)	Accurate for general inhomogeneity problems in gas mixtures	Inaccurate for multiphase mixing

distributions on the fly. Local k-g-distributions from the SGKs can be constructed in two formats, viz., full-spectrum and narrowband k-distributions. In the full-spectrum format, soot must be treated as gray and its spectrally averaged mean property (constant across spectrum) can then be added directly to full-spectrum k-distributions of the gas mixture. On the other hand, the narrowband format, allows consideration of nongray soot particles: absorption due to nongray soot can be added directly to the narrowband k-distributions of the gas mixture because the soot absorption coefficient is essentially constant across each narrowband (Modest and Riazzi, 2004).

In realistic combustion problems, soot is found to be present only close to the flame (locally), rather than everywhere in the domain (i.e., there are strong soot concentration

gradients in the domain). Also for almost all combustion flames, local peak soot volume fraction is in the order of parts-per-million amount, in which case the radiation from the gases is comparable to the radiation from the soot. For such a case, the accuracy of radiation calculations using single-scale FSK method can be severely challenged, whereas the MSFSK method has already been shown to accurately accommodate mixing of gas species with concentration gradient. Although mixing of nongray soot with gases has been performed using the single-scale FSK and SLW methods, additional problems are encountered when the MSFSK method is employed for inhomogeneous nongray gas–soot mixtures.

In the present work, we have extended out previous MSFSK method by incorporating nongray soot in the gas mixture. This is done by adding one more scale to the gas scales. This model is also designed to allow for both black and gray wall emission. In the previous model, wall emission was incorporated into the MSFSK method by distributing wall emission across all gas scales according to the absorption coefficient of each scale (Wang and Modest, 2007). Because wall emission is continuous in nature across the spectrum, similar to the radiation from soot, inclusion of wall emission in the soot scale is more appropriate. In order to mix molecular gases with nongray soot particles, the overlap parameters must be calculated at the narrowband level. First a brief mathematical discussion of the method is presented. Sample calculations are performed for a one-dimensional medium with step changes in species concentration and temperature and also for a two-dimensional axisymmetric medium involving combustion of methane. For all cases, results are compared to FSCK and LBL calculations.

MSFSK APPROACH FOR GAS-SOOT MIXTURES

A brief mathematical derivation of the MSFSK method is presented here. A participating medium containing molecular gases and nongray soot is considered. Scattering from the medium is assumed to be gray. The radiative heat transfer equation (RTE) for such a medium can be written as (Modest, 2003)

$$\frac{\mathrm{d}I_\eta}{\mathrm{d}s} = \kappa_\eta(\underline{\phi})I_{b\eta} - \left[\kappa_\eta(\underline{\phi}) + \sigma_s\right] I_\eta + \frac{\sigma_s}{4\pi}\int_{4\pi} I_\eta(\hat{s}')\Phi(\hat{s},\hat{s}')d\Omega' \tag{1}$$

subject to the boundary condition

$$\text{at} \quad s = 0: \quad I_\eta = \epsilon I_{b\eta w} + \frac{1-\epsilon}{\pi}\int_{2\pi} I_\eta|\hat{n}\cdot\hat{s}|\mathrm{d}\Omega \tag{2}$$

Here, I_η is the spectral radiative intensity, κ_η the absorption coefficient, $I_{b\eta}$ the spectral blackbody intensity (or Planck function), σ_s the gray scattering coefficient, Φ the scattering phase function, and wavenumber η is the spectral variable. The vector $\underline{\phi}$ contains

state variables that affect κ_η, which include temperature T, total pressure P, and gas mole fractions $\underline{x}$: $\underline{\phi} = (T, P, \underline{x})$. The boundary wall has been assumed to be gray and diffuse with ϵ being the emittance, $\hat{n}$ the surface normal, $\hat{s}$ the unit direction vector of incoming ray radiation, and Ω the solid angle. If one separates the contributions to κ_η from the M component gases and soot and breaks up the radiative intensity I_η accordingly, i.e.,

$$\kappa_\eta = \sum_{m=1}^{M} \kappa_{m\eta}, \qquad I_\eta = \sum_{m=1}^{M} I_{m\eta} \tag{3}$$

then the RTE Eq. (1) is transformed into M component RTEs, one for each species or scale. For each scale, this leads to

$$\begin{aligned} &\frac{\mathrm{d}I_{m\eta}}{\mathrm{d}s} = \kappa_{m\eta}(\underline{\phi}) I_{b\eta} - \left(\kappa_\eta(\underline{\phi}) + \sigma_s\right) I_{m\eta} + \frac{\sigma_s}{4\pi} \int_{4\pi} I_{m\eta}(\hat{s}')\Phi(\hat{s}, \hat{s}') d\Omega' \\ &\text{for } \; m = 1, \ldots, M \end{aligned} \tag{4}$$

It is observed that, physically, the intensity $I_{m\eta}$ for the mth scale is due to emission from the mth species but subject to absorption by all species.

It is important to note that, if there is no soot or wall emission present in the medium, the spectral locations where κ_η contributes to the absorption of $I_{m\eta}$ (i.e., absorption by all the gas scales) are only those wavenumbers for which $\kappa_{m\eta}$ is nonzero. Therefore, the overlap region is only a subset of those wavenumbers with $\kappa_{m\eta} \neq 0$, across which absorption from other gases occurs as well. The original MSFSK formulation takes advantage of the fact that the overlap regions for each scale are relatively small compared to the total emission/absorption spectrum of each scale (Zhang and Modest, 2002; Wang and Modest, 2005). In the presence of soot and wall emission, this assumption no longer holds. Hence, addition of soot radiation and wall emission into already-existing gas scales is not possible and an additional scale for soot radiation and wall emission is needed. Since radiation from soot and from wall emission are both continuous in nature both are combined into a single scale.

When all the wall emission is added to the soot scale, Eq. (2) can be written as

$$\text{at } \; s = 0 : \begin{cases} I_{m\eta} = \dfrac{1-\epsilon}{\pi} \displaystyle\int_{2\pi} I_{m\eta} \left|\hat{n}.\hat{s}\right| \mathrm{d}\Omega \quad \text{for } m = 1, \ldots, M-1 \;\; (\text{gas scales}) \\ I_{s\eta} = \epsilon I_{b\eta w} + \dfrac{1-\epsilon}{\pi} \displaystyle\int_{2\pi} I_{s\eta} \left|\hat{n}.\hat{s}\right| \mathrm{d}\Omega \;\; \text{for } \; s = M \;\; (\text{soot scale}) \end{cases} \tag{5}$$

where the subscript s denotes the soot scale.

We now apply the FSK scheme (Modest, 2003) to the RTE of each scale: First, Eq. (4) is multiplied by Dirac's δ function $\delta\left[k_m - \kappa_{m\eta}(\underline{\phi}_0)\right]$, followed by division with

$$f_m(T_0, \underline{\Phi}_0, k_m) = \frac{1}{I_b(T_0)} \int_0^\infty I_{b\eta}(T_0)\delta\left[k_m - \kappa_{m\eta}(\underline{\Phi}_0)\right] \mathrm{d}\eta \tag{6}$$

where $\underline{\Phi}_0$ and T_0 refer to a reference state. The resulting equation is then integrated over the entire spectrum, leading to

$$\frac{\mathrm{d}I_{mg}}{\mathrm{d}s} = k_m a_m I_b - \lambda_m I_{mg} + \frac{\sigma_s}{4\pi} \int_{4\pi} I_{mg}(\hat{s}')\Phi(\hat{s}, \hat{s}')d\Omega', \quad \text{for } m = 1, \ldots, M \tag{7}$$

where

$$I_{mg} = \int_0^\infty I_{m\eta}\delta\left[k_m - \kappa_{m\eta}\left(\underline{\Phi}_0\right)\right] \mathrm{d}\eta / f_m\left(T_0, \underline{\Phi}_0, k_m\right) \tag{8}$$

subscript g is the reordered spectrum and for the mth scale

$$g_m = \int_0^{k_m} f_m(T_0, \underline{\Phi}_0, k)\mathrm{d}k \tag{9}$$

a_m is the stretch factor for the mth scale (Modest and Zhang, 2002) and is written as

$$a_m = \frac{f_m(T, \underline{\Phi}_0, k_m)}{f_m(T_0, \underline{\Phi}_0, k_m)} \tag{10}$$

and λ_m is the overlap parameter of the mth scale with all other scales and can be written as

$$\lambda_m I_{mg} = k_m I_{mg} + \int_0^\infty \left(\sum_{n \neq m} \kappa_{n\eta}\right) I_{m\eta}\delta\left[k_m - \kappa_{m\eta}\left(\underline{\Phi}_0\right)\right] d\eta / f_m\left(T_0, \underline{\Phi}_0, k_m\right) \tag{11}$$

Similarly, FSK reordering is performed on boundary condition(s) with respect to $\kappa_{m\eta}(\underline{\Phi}_0)$, which results in

$$\text{at} \quad s = 0 : \begin{cases} I_{mg} = \dfrac{1-\epsilon}{\pi} \displaystyle\int_{2\pi} I_{mg} \left|\hat{n}.\hat{s}\right| \mathrm{d}\Omega \quad \text{for} \;\; m = 1, \ldots, M-1 \\ I_{sg} \;= \epsilon a_w I_{bw} + \dfrac{1-\epsilon}{\pi} \displaystyle\int_{2\pi} I_{sg} \left|\hat{n}.\hat{s}\right| \mathrm{d}\Omega \quad \text{for} \;\; s = M \end{cases} \tag{12}$$

where

$$I_{sg} = \int_0^\infty I_{s\eta}\delta\left(k_s - \kappa_{s\eta}\left(\underline{\Phi}_0\right)\right)\mathrm{d}\eta \Big/ f_s\left(T_0, \underline{\Phi}_0, k_s\right) \tag{13}$$

and a_w is the wall stretch factor for soot defined as

$$a_w = \frac{f_s(T_w, \underline{\Phi}_0, k_s)}{f_s(T_0, \underline{\Phi}_0, k_s)} \tag{14}$$

T_w is the wall temperature, which may be different from the medium temperature T.

The second term in Eq. (7) is due to the overlap of the absorption coefficient of the mth scale, $\kappa_{m\eta}$, with those of all other scales, which occurs over part of the spectrum. Details of the overlap parameter can be obtained from Zhang and Modest (2003). In the MSFSK method, the overlap parameter λ_m is evaluated in an approximate way, such that the emitted intensity emanating from a homogeneous nonscattering layer bounded by black walls is predicted exactly. The so-determined λ_m is a function of the state variables as well as of k_m (or g_m). Here, we follow the same approximate approach that was used in the original MSFSK development (Zhang and Modest, 2002; Wang and Modest, 2005).

In Eq. (7), the reordering is performed in terms of the scale absorption coefficients $\kappa_{m\eta}$ and the interaction between $\kappa_{m\eta}$ and κ_η during the reordering process is lumped into the overlap parameter λ_m. The reordering can also be performed in terms of κ_η, which, for a homogeneous layer at temperature T, leads to

$$\frac{\mathrm{d}I^*_{mg}}{\mathrm{d}s} = \frac{k^*_m I_b}{f(T, \underline{\Phi}, k)} - kI^*_{mg}, \quad \text{for } m = 1, \ldots, M \tag{15}$$

where

$$f(T, \underline{\Phi}, k) = \frac{1}{I_b(T)}\int_0^\infty I_{b\eta}(T)\delta\left[k - \kappa_\eta(\underline{\Phi})\right]\mathrm{d}\eta \tag{16}$$

$$I^*_{mg} = \int_0^\infty I_{m\eta}\delta\left(k - \kappa_\eta\left(\underline{\Phi}\right)\right)\mathrm{d}\eta \Big/ f\left(T, \underline{\Phi}, k\right) \tag{17}$$

$$k^*_m = \frac{1}{I_b}\int_0^\infty I_{b\eta}(T)\kappa_{m\eta}\delta\left[k - \kappa_\eta(\underline{\Phi})\right]\mathrm{d}\eta \tag{18}$$

Reordering boundary condition(s) with respect to $\kappa_\eta(\phi)$ leads to

$$\text{at } s=0: \begin{cases} I^*_{mg} = \dfrac{1-\epsilon}{\pi}\displaystyle\int_{2\pi} I^*_{mg}\,|\hat{n}.\hat{s}|\,\mathrm{d}\Omega \quad \text{for} \quad m=1,\ldots,M-1 \\ I^*_{sg} = \epsilon I_{bw}\dfrac{f\left(T_w,\underline{\phi},k\right)}{f\left(T,\underline{\phi},k\right)} + \dfrac{1-\epsilon}{\pi}\displaystyle\int_{2\pi} I^*_{sg}\,|\hat{n}.\hat{s}|\,\mathrm{d}\Omega \quad \text{for} \quad s=M \end{cases} \tag{19}$$

where

$$I^*_{sg} = \int_0^\infty I_{s\eta}\delta\left(k-\kappa_\eta\left(\underline{\phi}\right)\right)\mathrm{d}\eta \Big/ f\left(T,\underline{\phi},k\right) \tag{20}$$

In Eq. (15), the interaction between $\kappa_{m\eta}$ and κ_η is lumped into k^*_m. The solutions to Eqs. (7), (12), (15), and (19) for a homogeneous layer at temperature T bounded by black walls can be obtained analytically, and the total exiting intensities from the gas scales at $s=L$ are

$$\begin{aligned} I_m &= \int_0^1 I_{mg}\mathrm{d}g = \int_0^\infty \frac{k_m}{\lambda_m} I_b[1-\exp(-\lambda_m s)]\, f_m(T,\underline{\phi},k_m)\mathrm{d}k_m \\ &\text{for } m=1,\ldots,M-1 \end{aligned} \tag{21}$$

and

$$I^*_m = \int_0^1 I^*_{mg}\mathrm{d}g = \int_0^\infty \frac{k^*_m}{k} I_b\left[1-\exp(-ks)\right]\mathrm{d}k, \quad \text{for } m=1,\ldots,M-1 \tag{22}$$

respectively. Because wall emission is added to the soot scale, total exiting intensity from the soot scale at $s=L$ is

$$\begin{aligned} I_s &= \int_0^1 I_{sg}\mathrm{d}g = \int_0^\infty a_w I_{bw}\exp(-\lambda_s L) f_s(T,\underline{\phi},k_s)\mathrm{d}k_s \\ &+ \int_0^\infty \frac{k_s}{\lambda_s} I_b\left[1-\exp(-\lambda_s L)\right] f_s(T,\underline{\phi},k_s)\mathrm{d}k_s = I_{s1}+I_{s2} \end{aligned} \tag{23}$$

where I_{s1} is short-hand for the first term (wall emission), and I_{s2} for the second term (medium emission) and

$$\begin{aligned} I_s^* &= \int_0^1 I_{sg}^* \mathrm{d}g = \int_0^\infty I_{bw} f(T_w, \underline{\phi}, k) \exp(-kL) \mathrm{d}k \\ &+ \int_0^\infty \frac{k^*}{k} I_b \left[1 - \exp(-kL)\right] \mathrm{d}k = I_{s1}^* + I_{s2}^* \end{aligned} \tag{24}$$

where again I_{s1}^* abbreviates the first term (wall emission), and I_{s2}^* the second term (medium emission).

The spectrally integrated intensity, I_m, should be equal to I_m^* (for gas scales), and I_s, should be equal to I_s^* (for the soot scale). For gas scales, this requirement leads to

$$\lambda_m = k \quad \text{and} \quad k_m f_m(T, k_m) \mathrm{d}k_m = k_m^*(k) \mathrm{d}k \tag{25}$$

or

$$k_m^*(\lambda_m) \mathrm{d}\lambda_m = k_m f_m(T, k_m) \mathrm{d}k_m \tag{26}$$

Similar to the original MSFSK method, Eq. (26) provides the relationship between λ_m and k_m that is required to solve Eq. (7). One convenient way of determining λ_m is using the relationship [7]

$$\int_0^{k_m} k_m f_m(T, k_m) \mathrm{d}k_m = \int_0^{k=\lambda_m} k_m^*(k) \mathrm{d}k \tag{27}$$

For the soot scale, we use the strategy that the overlap parameter λ_s is determined by equating medium emission I_{s2} and I_{s2}^*, as was done in the original MSFSK formulation. This leads to the same equation as Eq. (27). To equate overall intensity from the soot scale, the wall emissions I_{s1} and I_{s1}^* must also be equal. The expression for I_{s1}^* is rearranged employing the approximation for λ_s, Eq. (26),

$$\begin{aligned} I_{s1}^* &= \int_0^\infty \frac{f(T_w, \underline{\phi}, k)}{k_s^*(T, \underline{\phi}, k)} k_s^*(T, \underline{\phi}, k) I_{bw} \exp(-kL) \mathrm{d}k \\ &= \int_0^\infty \frac{f(T_w, \underline{\phi}, \lambda_s)}{k_s^*(T, \underline{\phi}, \lambda_s)} k_s(T, \underline{\phi}) I_{bw} \exp(-\lambda_s L) f_s(T, \underline{\phi}, k_s) \mathrm{d}k_s \end{aligned} \tag{28}$$

By comparison to the expression for I_{s1} in Eq. (23), it is clear that if

$$a_w = \frac{f(T_w, \underline{\phi}, \lambda_s)}{k_s^*(T, \underline{\phi}, \lambda_s)} k_s(T, \underline{\phi}) \tag{29}$$

then I_{s1} equals I_{s1}^*.

Evaluation of Overlap Parameter

The overlap parameter is determined efficiently and accurately from a database of narrowband (NB) k-distributions of individual species (scales). The advantages of using NB k-distributions are that assembling mixture FS $k$distributions from NB k-distributions of individual gas species mixed at the narrowband level is more accurate than mixing entire FS k-distributions of individual species. In addition, the use of NB k-distributions of individual species allows the inclusion of nongray absorbing particles in the participating medium (Modest and Riazzi, 2004).

For the mth scale, substituting Eq. (18), the right-hand side (RHS) of Eq. (27) may be rewritten in terms of narrowband k^*_m

$$\text{RHS} = \int_0^{k=\lambda_m} \sum_{i=1}^{N_{\text{nb}}} \frac{I_{bi}}{I_b} \frac{1}{\Delta\eta} \int_{\Delta\eta} \kappa_{m\eta} \delta(k-\kappa_\eta) \mathrm{d}\eta \, \mathrm{d}k = \sum_{i=1}^{N_{\text{nb}}} \frac{I_{bi}}{I_b} \int_0^{k=\lambda_m} k^*_{m,i}(k) \mathrm{d}k \tag{30}$$

where $k^*_{m,i}$ is the narrowband counterpart of k^*_m, N_{nb} is the number of narrowbands comprising the entire spectrum, and the NB Planck function I_{bi} is defined as

$$I_{bi} = \int_{\Delta\eta} I_{b\eta} \mathrm{d}\eta \tag{31}$$

As always in the NB k-distribution approach, we have assumed that $I_{b\eta}$ is constant over $\Delta\eta$ and can be approximated by $I_{bi}/\Delta\eta$.

In order to evaluate the integrals involving $k^*_{m,i}$ in Eq. (30) in terms of NB k-distributions, we consider the quantity Q_m

$$Q_m = \frac{1}{\Delta\eta} \int_{\Delta\eta} \kappa_{m\eta} \exp(-\kappa_\eta L) \mathrm{d}\eta \tag{32}$$

for the ith narrowband. Physically, Q_m is related to narrowband emission from scale m, attenuated over path L by the entire gas mixture. Q_m can be rewritten as

$$\begin{aligned} Q_m &= \frac{1}{\Delta\eta} \int_{\Delta\eta} \kappa_{m\eta} \int_0^\infty \exp(-kL) \delta(k-\kappa_\eta) \mathrm{d}k \, \mathrm{d}\eta \\ &= \int_0^\infty k^*_{m,i} \exp(-kL) \mathrm{d}k = \mathcal{L}(k^*_{m,i}) \end{aligned} \tag{33}$$

i.e., Q_m is the Laplace transform of $k^*_{m,i}$.

Previously, it has been shown that, on a narrowband basis, the spectral behavior of different species is essentially statistically uncorrelated, while the soot absorption coefficient is essentially constant across each narrowband (Modest and Riazzi, 2004; Wang and Modest, 2005). With these two assumptions for the soot scale, Q_m can also be written as (using subscript $m = s$)

$$Q_s \approx \overline{k}_{s,i} \exp(-\overline{k}_{s,i} L) \prod_{n \neq s} \left(\frac{1}{\Delta\eta} \int_{\Delta\eta} \exp(-\kappa_{n\eta} L) \mathrm{d}\eta \right) \tag{34}$$

where $k_{s,i}$ is the NB average value of the soot absorption coefficient. The k-distribution method can then be applied to Eq. (34) and we obtain

$$\begin{aligned} Q_s &\approx \overline{k}_{s,i} \exp(-\overline{k}_{s,i} L) \prod_{n \neq s} \left[\int_0^1 \exp(-k_{n,i} L) \mathrm{d}g_n \right] \\ &= \int_{g_{1,i}=0}^{1} \cdots \int_{g_{M-1,i}=0}^{1} \overline{k}_{s,i} \exp\left(-\overline{k}_{s,i} L - \sum_{n \neq s} k_{n,i} L \right) \mathrm{d}g_{M-1,i} \ldots \mathrm{d}g_{1,i} \end{aligned} \tag{35}$$

Equating Eqs. (33) and (35), we have

$$\mathcal{L}(k^*_{s,i}) \approx \int_{g_{1,i}=0}^{1} \cdots \int_{g_{M-1,i}=0}^{1} \overline{k}_{s,i} \exp\left(-\overline{k}_{s,i} L - \sum_{n \neq s} k_{n,i} L \right) \mathrm{d}g_{M-1,i} \ldots \mathrm{d}g_{1,i} \tag{36}$$

and, using the integral property of the Laplace transform,

$$\begin{aligned} \mathcal{L}\left[\int_0^{k=\lambda_s} k^*_{s,i}(k) \mathrm{d}k \right] \approx & \int_{g_{1,i}=0}^{1} \cdots \int_{g_{M-1,i}=0}^{1} \overline{k}_{s,i} \frac{\exp\left(-\overline{k}_{s,i} L - \sum\limits_{n \neq s} k_{n,i} L \right)}{L} \\ & \times \mathrm{d}g_{M-1,i} \ldots \mathrm{d}g_{1,i} \end{aligned} \tag{37}$$

Finally, taking the inverse Laplace transform, we obtain

$$\begin{aligned} \int_0^{k=\lambda_s} k^*_{s,i}(k) \mathrm{d}k \approx & \overline{k}_{s,i} \int_{g_{1,i}=0}^{1} \cdots \int_{g_{M-1,i}=0}^{1} H\left(\lambda_s - \overline{k}_{s,i} - \sum_{n \neq s} k_{n,i} \right) \\ & \times \mathrm{d}g_{M-1,i} \ldots \mathrm{d}g_{1,i} \end{aligned} \tag{38}$$

where H is the Heaviside step function.

For the mth gas scale, using the same approach, we obtain

$$\int_0^{k=\lambda_m} k^*_{m,i}(k)\mathrm{d}k \approx \int_{g_{1,i}=0}^{1} \dots \int_{g_{M-1,i}=0}^{1} k_{m,i} H\left(\lambda_m - \overline{k}_{s,i} - \sum_{n\neq s} k_{n,i}\right) \mathrm{d}g_{M-1,i} \dots \mathrm{d}g_{1,i} \quad (39)$$

The left-hand side (LHS) of Eq. (27) is also readily expressed in terms of NB k-distributions for the mth scale as

$$\begin{aligned} \text{LHS} &= \int_0^{k_m} k_m \frac{1}{I_b} \int_0^{\infty} I_{b\eta}\delta(k_m - \kappa_{m\eta})\mathrm{d}\eta \, \mathrm{d}k_m \\ &= \sum_{i=1}^{N_{\text{nb}}} \frac{I_{bi}}{I_b} \int_0^{k_m} k_m \frac{1}{\Delta\eta} \int_{\Delta\eta} \delta(k_m - \kappa_{m\eta})\mathrm{d}\eta \, \mathrm{d}k_m = \sum_{i=1}^{N_{\text{nb}}} \frac{I_{bi}}{I_b} \int_0^{g_{m,i}(k_m)} k_{m,i}\mathrm{d}g_{m,i} \end{aligned} \quad (40)$$

Equating the LHS and RHS, we obtain a generic expression for the determination of the overlap parameter λ_m of the mth gas scale based on NB k-distributions of individual gas species as

$$\sum_{i=1}^{N_{\text{nb}}} \frac{I_{bi}}{I_b} \int_0^{g_{m,i}(k_m)} k_{m,i}\mathrm{d}g_{m,i} = \sum_{i=1}^{N_{\text{nb}}} \frac{I_{bi}}{I_b} \int_{g_{1,i}=0}^{1} \dots \int_{g_{M-1,i}=0}^{1} k_{m,i} H\left(\lambda_m - \overline{k}_{s,i} - \sum_{n\neq s} k_{n,i}\right)$$

$$\times \, \mathrm{d}g_{M-1,i} \dots \mathrm{d}g_{1,i} \quad \text{for} \quad m = 1 \dots M-1 \quad (41)$$

For the soot scale, λ_s is evaluated from

$$\sum_{i=1}^{N_{\text{nb}}} \frac{I_{bi}}{I_b} \int_0^{g_{s,i}(k_s)} k_{s,i}\mathrm{d}g_{s,i} = \sum_{i=1}^{N_{\text{nb}}} \frac{I_{bi}}{I_b} \overline{k}_{s,i} \int_{g_{1,i}=0}^{1} \dots \int_{g_{M-1,i}=0}^{1} H\left(\lambda_s - \overline{k}_{s,i} - \sum_{n\neq s} k_{n,i}\right)$$

$$\times \, \mathrm{d}g_{M-1,i} \dots \mathrm{d}g_{1,i} \qquad s = \text{soot scale} \quad (42)$$

The integrals in Eqs. (41) and (42) can be evaluated efficiently based on the narrowband database compiled by Wang and Modest (2005b), as was shown by Wang and Modest (2005a).

Evaluation of Modified Wall Stretch Factor

Incorporation of wall emission into the soot scale, Eq. (12), introduces the stretch factor a_w in the MSFSK formulation. The parameter a_w can be evaluated in two ways: from the direct definition, Eq. (14), and from the modified definition, Eq. (29). MSFSK calculations using the directly calculated a_w may not recover the LBL result for a homogeneous medium bounded by a gray wall at a different temperature from that of the medium, due to the approximation made for λ_s. On the other hand, MSFSK calculations using the modified a_w from Eq. (29) recover the LBL result for homogeneous media with arbitrary boundary wall temperatures because it is formulated to incorporate the approximation made for λ_s. If the gas is nonisothermal, then the modified a_w is evaluated at the reference temperature.

The narrowband k-distributions constructed by Wang and Modest (2005b) are used to calculate the wall stretch factor for both cases–direct and modified. Calculation of the modified a_w, from Eq. (29), requires evaluation of k_s^* and $f(T_w, \underline{\phi}, \lambda_s)$. k_s^* can be determined by differentiating the RHS of Eq. (27), which must be calculated for the determination of λ_s. This approach is found to be accurate and robust and is implemented as follows: the RHS is calculated from the RHS of Eq. (42) for a set of λ_s values using the narrowband database; because it is a monotonically increasing function of λ_s, a monotonic cubic spline can be constructed readily; then, the polynomial coefficients for the first-order term are the k_s^* for the corresponding λ_s values (Wang and Modest, 2005). For the calculation of $f(T_w, \underline{\phi}, \lambda_s)$, the soot absorption coefficient must be mixed with gas-absorption coefficients at the narrowband level. Details of this method can be found in Modest and Riazzi (2004). Then, $f(T_w, \underline{\phi}, \lambda_s)$ is evaluated using the Planck function at the wall temperature.

SAMPLE CALCULATIONS

1D Problem

To demonstrate the performance of the new MSFSK model for gas–soot mixtures, first a one-dimensional medium containing CO_2–H_2O–N_2 with and without soot, confined between cold black walls, is considered. The mixture consists of two different homogeneous layers (denoted as left and right layer/column) adjacent to each other at a total pressure of 1 bar, with a step jump in the concentrations of the species. The temperature of both layers are either the same, or an additional step jump in temperature is introduced. Two different cases are considered for radiation calculation in such a 1D medium: *(i)* the right layer has a fixed width of 50 cm, while the width of the left layer is varied in the calculations; *(ii)* the left layer has a fixed width of 50 cm, while the width of the right layer is varied in the calculations. Only emitting/absorbing (nonscattering) soot is considered in sample calculations, as would be the case for nonagglomerated soot.

This approximation is invoked in most predictions of radiative transfer in gas/soot mixtures (Solovjov and Webb, 2001). The radiative heat flux leaving from the right layer is calculated using the LBL method, the single-scale FSCK method, and the new MSFSK method. The errors are calculated with respect to the benchmark LBL calculations. Such problems with steps in species concentration and/or temperature provide an acid test for these methods because of their extreme inhomogeneity gradients.

First, we investigate the case where the right layer has a fixed width of 50 cm, while the width of the left layer is varied. Figure 1 shows the results for such a case of gas-soot mixture with a step change in concentration in the gas scales. The soot is uniform (0.1 ppm) throughout. It is observed that for both temperatures MSFSK calculations predict heat flux more accurately than the FSCK method. For the lower temperature

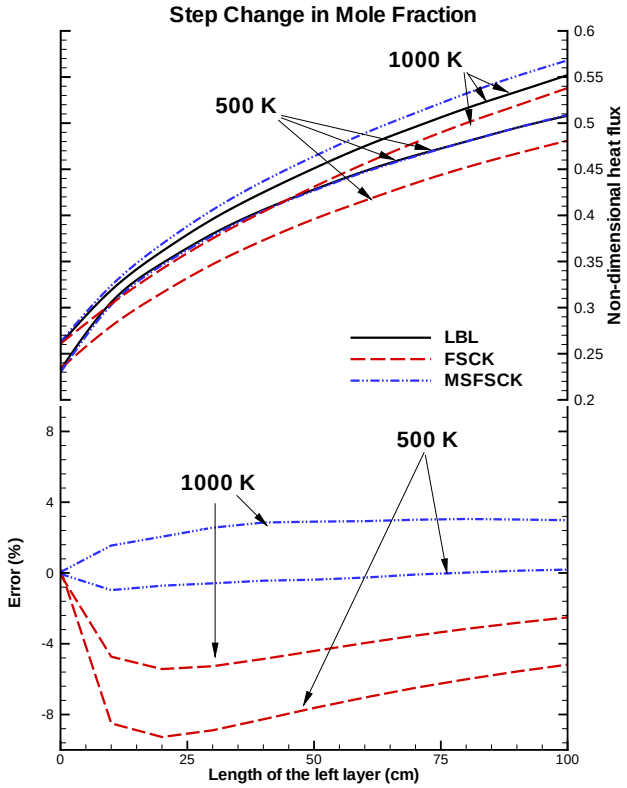

Figure 1. Nondimensional heat flux leaving an inhomogeneous slab at a total pressure of 1 bar, with step changes in mole fraction of gas species: left layer contains 2% CO_2, 20% H_2O, and 0.1 ppm soot; right layer contains 20% CO_2, 2% H_2O, and 0.1 ppm soot

(500 K), the maximum error in the MSFSK calculations is limited to 1%, whereas for 1000 K the maximum error is 3.5%. On the other hand, the maximum error for the FSCK method is 10% and 5.5% for 500 and 1000 K, respectively.

Next we perform radiation calculations for the case where the left layer has a fixed width of 50 cm, while the width of the right layer is varied. Figure 2 shows the results for a case of gas–soot mixture including mole fraction step changes in all the three scales (species). In this inhomogeneous problem, the error of the single-scale FSCK method reaches $>$ 26% for the 500 K case and 14% for the 1500 K case. In comparison to that, if the gas–soot mixture is broken into several scales, one for each species, the new MSFSK method produce more accurate solutions, with maximum errors limited to 3% for the 500 K case and 4% for the 1500 K case.

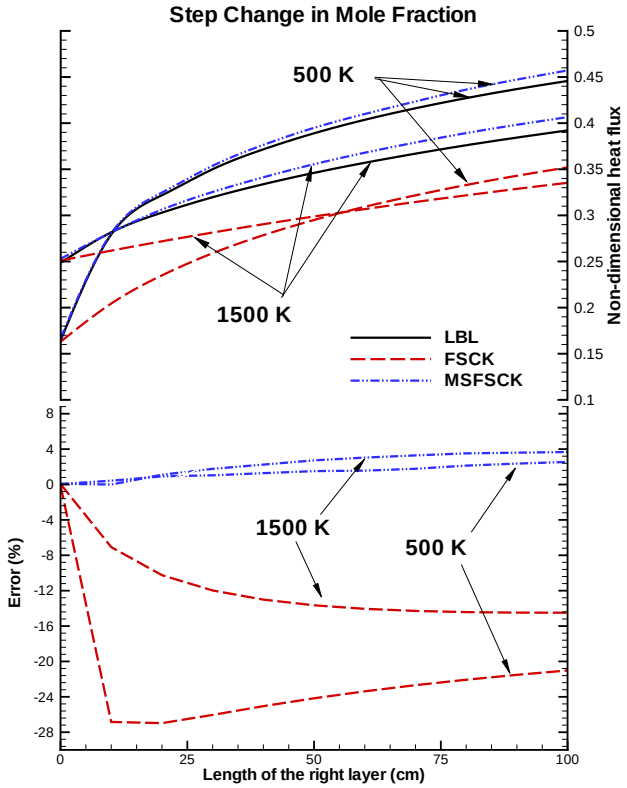

Figure 2. Nondimensional heat flux leaving an inhomogeneous slab at a total pressure of 1 bar, with step changes in mole fraction: left layer contains 20% CO_2 and 0.1 ppm soot; right layer contains 20% H_2O

After performing tests with step changes in concentration only for the 1D problem, we now also introduce step changes in temperature. The left and right layers are now at 1500 and 1000 K, respectively. Two different cases are considered. In case 1, the left layer contains 2% CO_2, 20% H_2O, and 0.1 ppm soot and the right layer contains 20% CO_2, 2% H_2O, and no soot; Case 2: the concentrations are exactly reversed from the previous case (i.e., the left layer contains 20% CO_2, 2% H_2O, and no soot and the right layer contains 2% CO_2, 20% H_2O and 0.1 ppm soot). Figure 3 shows that MSFSK calculations are more accurate than the single-scale FSCK results. For Case 1, the maximum error in the MSFSK calculations is limited to 4% while the FSCK method incurs a maximum error of 10%. For Case 2, the maximum MSFSK error is 8% while the maximum FSCK error is 16%. Although this MSFSK method has been developed to accommodate mixing

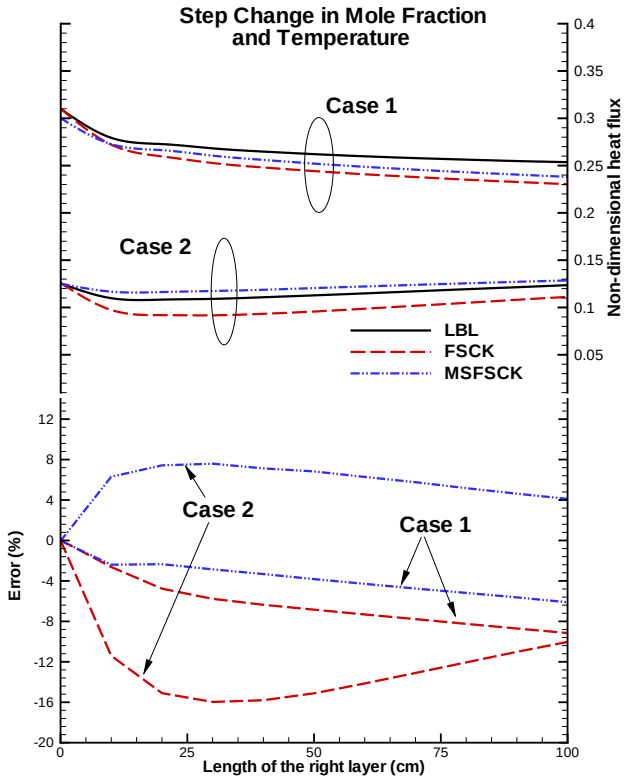

Figure 3. Nondimensional heat flux leaving an inhomogeneous slab at a total pressure of 1 bar, with step changes in mole fraction and temperature: left layer contains 2% CO_2, 20% H_2O, and 0.1 ppm soot at 1500 K; right layer contains 20% CO_2, 2% H_2O, and no soot at 1000 K

and concentration inhomogeneity problems, it is observed that breaking up the mixture into scales (species) helps to reduce error in temperature inhomogeneities as well. 1D problems with wall emission are investigated in Figs. 4 and 5. Figure 4 shows results for the case where both layers are at 1000 K; the length of both the left and the right layers are kept at 50 cm while the wall temperature of the left layer is varied. Gray wall emission is considered, and the wall emittance is taken as $\epsilon = 0.6$. Step changes in concentration are introduced in all scales. A comparison is made between LBL, single-scale FSCK, MSFSK [with direct calculation of a_w from Eq. (14)], and MSFSK [with calculation using the modified a_w from Eq. (29)]. It is observed that MSFSK calculations with modified a_w are the most accurate (maximum error of 2%). MSFSK calculations with

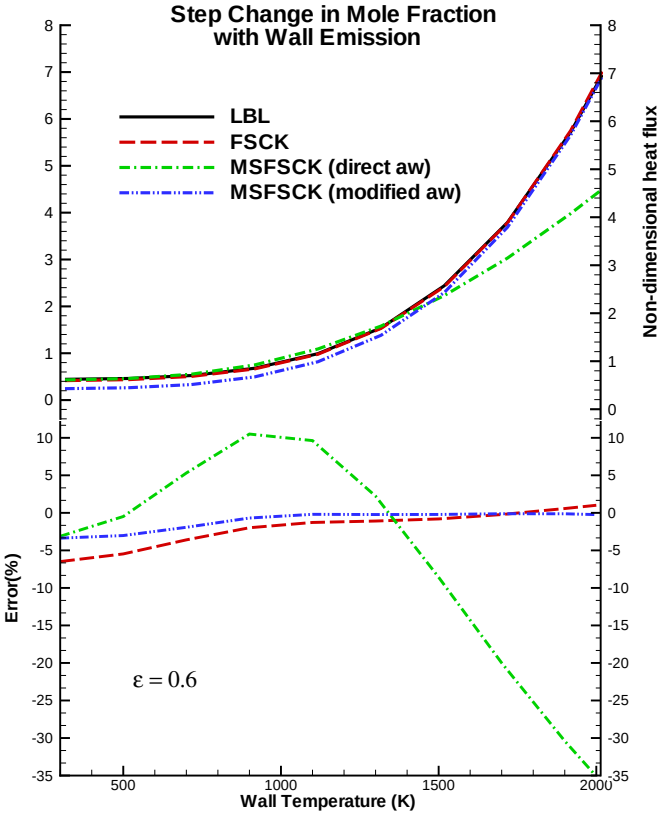

Figure 4. Nondimensional heat flux leaving an inhomogeneous slab at a total pressure of 1 bar, with wall emission and step changes in mole fraction: left layer contains 20% CO_2, 2% H_2O, and 0.1 ppm soot; right layer contains 2% CO_2, 20% H_2O, and no soot; both layers at 1000 K

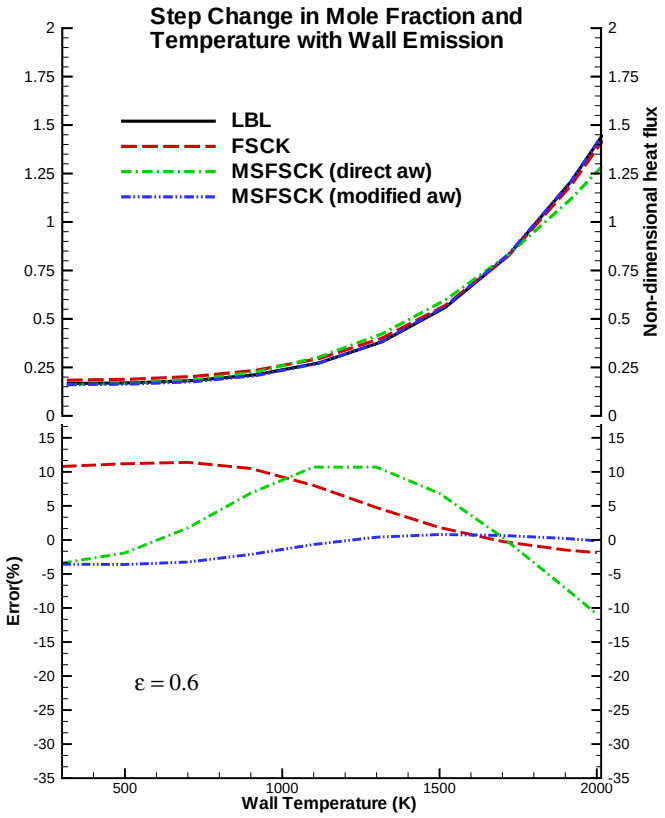

Figure 5. Nondimensional heat flux leaving an inhomogeneous slab at a total pressure of 1 bar, with wall emission, step changes in mole fraction and temperature: left layer contains 2% CO_2, 20% H_2O, and no soot at 1500 K; right layer contains 20% CO_2, 2% H_2O, and 0.1 ppm soot at 1000 K

direct a_w cannot recover the intensity emitted by a homogeneous medium surrounded by black wall and, hence, can become very inaccurate for very disparate layers. Although the single-scale FSCK method incurs larger errors at low temperature (maximum error of 6%), it performs much better at higher wall temperatures, i.e. when wall emission becomes dominant compared to radiation from the medium and, hence, single-scale FSCK calculations provide close-to-LBL accuracy.

Figure 5 shows results for a 1D problem similar to Fig. 4 but with concentrations reversed from the previous case and also including a step change in temperature, with temperatures of the left and the right layers at 1500 and 1000 K, respectively. It is again observed that MSFSK calculations with modified a_w performs best with a maximum error of 3% at low wall temperatures, whereas the FSCK method has $> 10\%$ error.

2D Problem

Next we consider a more realistic, but still severe, 2D problem of the axisymmetric methane burner considered by Modest and Zhang during the development of the FSCK method (2002), with its sharp temperature and (independently varying) concentration gradients. In that work a pure gas mixture was considered, whereas here soot will be added to the gas mixture. The soot volume fraction is obtained from a state relationship for the fuel–air equivalence ratio (Mazumder, 1997). Temperature and concentration distributions for CO_2, H_2O, and CH_4 can be obtained from previous work by Modest and Zhang (2002). The distribution of the soot volume fraction is shown in Fig. 6 and shows some discontinuities caused by slight wiggles in concentration, which are greatly amplified by the state relationship. The local radiative heat source term is calculated using LBL, FSCK, and MSFSK approaches, employing the P-1 method as the RTE solver, and relative errors are determined by comparison to LBL as

$$\text{error}(\%) = \frac{\nabla.q_{\text{LBL}} - \nabla.q_{\text{FSCK/MSFSK}}}{\nabla.q_{\text{LBL,max}}} \times 100 \tag{43}$$

Figure 7 shows that the single-scale FSCK method generates large errors for gas–soot mixtures with varying ratios of concentrations (the maximum error in the present problem reaches as much as 30% near the inlet). In the multiscale approach, CO_2 and H_2O are combined into a single scale because they have the same ratio of concentration throughout the combustion chamber, whereas CH_4 is treated as a second scale. The maximum error is now limited to 7% near the inlet (region of high errors) as seen in Fig. 8. This is a substantial improvement, and the accuracy of the new MSFSK approach

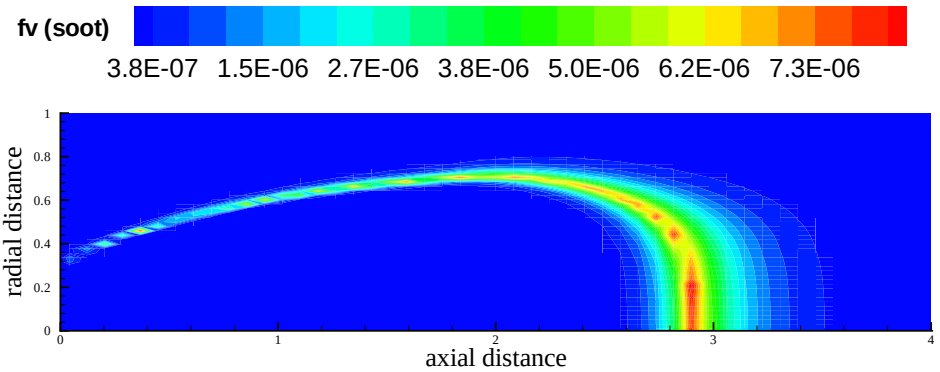

Figure 6. Distribution of soot volume fraction for 2D test flame

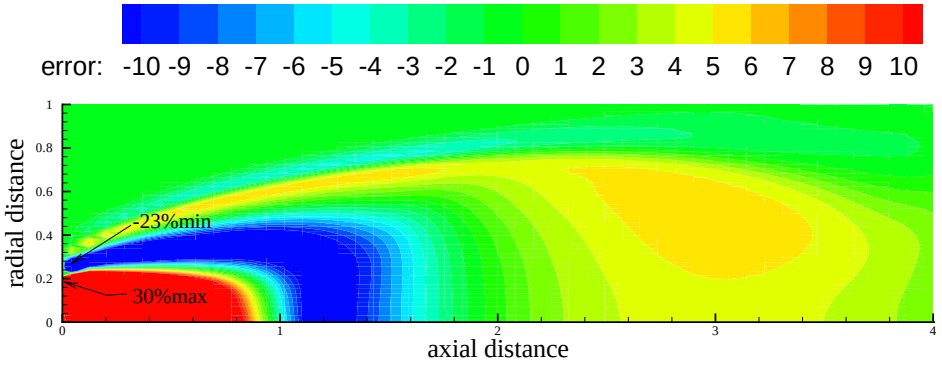

Figure 7. Relative error for radiative heat source calculations using single-scale FSCK compared to LBL in a gas (CO_2, H_2O, CH_4)–soot mixture in 2D combustion chamber

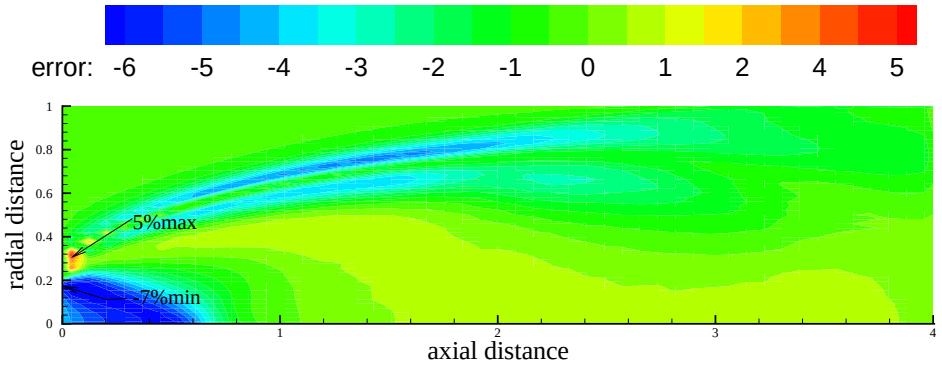

Figure 8. Relative error for radiative heat source calculations using MSFSK compared to LBL in a gas (CO_2, H_2O, CH_4)–soot mixture in 2D combustion chamber

for gas–soot mixtures is clearly demonstrated. CPU time for the LBL calculations is 55 h on a 2.4 GHz AMD Opteron machine, while the single-scale FSK and modified MSFSK take only 5 and 30 sec (which is typically of the same order as finite volume solutions of the flow field and chemistry in a combustion problem), respectively, for this calculation. This implies factors of 4×10^4 and 7×10^3 CPU savings, respectively, compared to LBL.

CONCLUSION

In this paper, a new multiscale full-spectrum k-distribution method has been developed for radiation calculations involving nongray gas–soot mixtures with gray wall emission.

Because of the continuous nature of both, wall emission and radiation from soot, they are lumped into a single scale. Sample calculations are performed for both 1D and 2D media for gas–soot mixtures with and without wall emission. The MSFSK method is more accurate than the single-scale FSCK method, observed to efficiently mix gases with soot, and accurately predicts radiative fluxes in the presence concentration inhomogeneities. The MSFSK method with modified wall stretch factor produces close to line-by-line accuracy. It is seen that, at higher wall temperatures, when wall emission dominates over radiation from the medium, use of single-scale FSCK can produce sufficiently accurate results. In realistic combustion problems, the multiscale method is able to provide very accurate results (an order of magnitude more accurate than the FSCK with several orders of magnitude less computational cost than LBL). The modified MSFSK method can be easily used with any RTE solver within the framework of existing CFD code facilitating combustion calculations with radiation feedback.

REFERENCES

Denison, M. K. and Webb, B. W., A spectral line based weighted-sum-of-gray-gases model for arbitrary RTE solvers, *ASME J. Heat Transfer*, vol. 115, pp. 1004-1012, 1993.

Denison, M. K. and Webb, B. W., The spectral-line-based weighted-sum-of-gray-gases model in nonisothermal nonhomogeneous media, *ASME J. Heat Transfer*, vol. 117, pp. 359-365, 1995.

Rivière, Ph., Soufiani, A., Perrin, M. Y., Riad, H., and Gleizes, A., Air mixture radiative property mdelling in the temperature range 1000040000 K, *J. Quant. Spectrosc. Radiat. Transfer*, vol. 56, pp. 29-45, 1996.

Pierrot, L., Rivière, Ph., Soufiani, A., and Taine, J., A fictitious-gas-based absorption distribution function global model for radiative transfer in hot gases, *J. Quant. Spectrosc. Radiat. Transfer*, vol. 62, pp. 609-624, 1999.

Modest, M. F. and Zhang, H., The full-spectrum correlated k-distribution for thermal radiation from molecular gasparticulate mixtures, *ASME J. Heat Transfer*, vol. 124, pp. 30-38, 2002.

Modest, M. F. and Riazzi, R. J., Assembly of full-spectrum k-distributions from a narrowband database; efects of mixing gases, gases and nongray absorbing particles, and mixtures with nongray scatterers in nongray enclosures, *J. Quant. Spectrosc. Radiat. Transfer*, vol. 90, pp. 169-189, 2004.

Zhang, H. and Modest, M. F., A multi-scale full-spectrum correlated k-distribution for radiative heat transfer in inhomogeneous gas mixtures, *J. Quant. Spectrosc. Radiat. Transfer*, vol. 73, pp. 349-360, 2002.

Zhang, H. and Modest, M. F., Scalable multi-group full-spectrum correlated k-distributions for radiative heat transfer, *ASME J. Heat Transfer*, vol. 125, pp. 454-461, 2003a.

Zhang, H. and Modest, M. F., Multi-group full-spectrum k-distribution database for water vapor mixtures in radiative transfer calculations, *Int. J. Heat Mass Transfer*, vol. 46, pp. 3593-3603, 2003b.

Wang, L. and Modest, M. F., Narrowband based multiscale full-spectrum k-distribution method for radiative transfer in inhomogeneous gas mixtures, *ASME J. Heat Transfer*, vol. 127, pp. 740-748, 2005a.

Pal, G. and Modest, M. F., A new hybrid full-spectrum correlated k-distribution method for radiative transfer calculations in nonhomogeneous gas mixtures, In *2007 ASME-JSME Thermal Engineering Conference and Summer Heat Transfer Conference*, 2007.

Pal, G., Modest, M. F., and Wang, L., Hybrid full-spectrum correlated k-distribution method for radiative transfer in strongly nonhomogeneous gas mixtures, *ASME J. Heat Transfer*, (submitted), 2007.

Wang, L., Haworth, D. C., Turns, S. R., and Modest, M. F., Interactions among soot, thermal radiation, and NOx emissions in oxygen-enriched turbulent nonpremixed flames: a CFD modeling study, *Combust. Flame*, vol. 141, pp. 170-179, 2005.

Solovjov, V. and Webb, B. W., An efficient method of modeling radiative transfer in multicomponent gas mixtures with soot, *ASME J. Heat Transfer*, vol. 123, pp. 450-457, 2001.

Wang, L., Modest, M. F., Haworth, D. C., and Turns, S. R., Modeling nongray soot and gas-phase radiation in luminous turbulent nonpremixed jet flames, *Combust. Theory Model.*, vol. 9, pp. 479-498, 2005.

Wang, L. and Modest, M. F., Treatment of wall emission in the narrow-band based multiscale full-spectrum k-distribution method, *ASME J. Heat Transfer*, vol. 129, pp. 743-748, 2007.

Modest, M. F., Radiative Heat Transfer, 2nd ed, Academic Press, New York, 2003a.

Modest, M. F. Narrowband and full-spectrum k-distributions for radiative heat transfercorrelated-k vs. scaling approximation, *J. Quant. Spectrosc. Radiat. Transfer*, vol. 76, pp. 69-83, 2003b.

Wang, A. and Modest, M. F., High-accuracy, compact database of narrow-band k-distributions for water vapor and carbon dioxide, *J. Quant. Spectrosc. Radiat. Transfer*, vol. 93, pp. 245-261, 2005b.

Mazumder, S. *Numerical Study of Chemically Reactive Turbulent Flows with Radiative Heat Transfer*, Ph.D. Thesis, The Pennsylvania State University, University Park, PA, 1997.